J|A|C|S
ARTICLES
Published on Web 11/21/2002

Probing the Reactivity of Photoinitiators for Free Radical Polymerization: Time-Resolved Infrared Spectroscopic Study of Benzoyl Radicals

Christopher S. Colley,[†] David C. Grills,[†] Nicholas A. Besley,[†] Steffen Jockusch,[‡] Pavel Matousek,[§] Anthony W. Parker,[§] Michael Towrie,[§] Nicholas J. Turro,[‡] Peter M. W. Gill,[†] and Michael W. George*,[†]

Contribution from the School of Chemistry, University of Nottingham, University Park, Nottingham, NG7 2RD, United Kingdom, Department of Chemistry, Columbia University, New York, New York 10027, and Central Laser Facility, CLRC Rutherford Appleton Laboratory, Chilton, Didcot, Oxfordshire, OX11 0QX, United Kingdom

Received March 5, 2002

Abstract: A series of substituted benzoyl radicals has been generated by laser flash photolysis of α-hydroxy ketones, α-amino ketones, and acyl and bis(acyl)phosphine oxides, all of which are used commercially as photoinitiators in free radical polymerizations. The benzoyl radicals have been studied by fast time-resolved infrared spectroscopy. The absolute rate constants for their reaction with *n*-butylacrylate, thiophenol, bromotrichloromethane and oxygen were measured in acetonitrile solution. The rate constants of benzoyl radical addition to *n*-butylacrylate range from 1.3×10^5 to 5.5×10^5 M^{-1} s^{-1} and are about 2 orders of magnitude lower than for the *n*-butylacrylate addition to the counterradicals that are produced by α-cleavage of the investigated ketones. Density functional theoretical calculations have been performed in order to rationalize the observed reactivities of the initiating radicals. Calculations of the phosphorus-centered radicals generated by photolysis of an acyl and bis(acyl)phosphine oxide suggest that P atom Mulliken spin populations are an indicator of the relative reactivities of the phosphorus-centered radicals. The α-cleavage of (2,4,6-trimethylbenzoyl)phosphine oxide was studied by picosecond pump−probe and nanosecond step-scan time-resolved infrared spectroscopy. The results support a mechanism in which the α-cleavage occurs from the triplet excited state that has a lifetime less than or equal to the singlet excited state.

Introduction

Aryl ketones, such as α-hydroxy ketones (**1a**, **2a**), α-amino ketones (**3a**, **4a**), and acyl and bis(acyl)phosphine oxides (**5a** and **6a**, respectively), have been widely used as photoinitiators in free radical polymerizations.[1−4] Upon irradiation these ketones undergo classical type I cleavage to produce radical pairs with a high rate constant and good efficiency (eqs 1−6).[5−12] The addition of the radicals (**1b**−**6b**, **1c**−**6c**) to alkenes (initiation step) is one of the most important reactions in free radical polymerization. Consequently, the factors controlling the rate constants have been the subject of much experimental and theoretical work. Laser flash photolysis with transient UV/visible detection was employed to determine the addition rate constants to alkenes for the radicals **1c**−**6c**.[13−16] Unfortunately, the benzoyl radicals **1b**−**6b** have low extinction coefficients at wavelengths higher than 300 nm and are therefore difficult to detect directly by their UV/visible absorption bands; e.g., the unsubstituted benzoyl radical **1b** exhibits a weak transient absorption at 368 nm ($\epsilon \approx 150$ M^{-1} cm^{-1}).[17,18] In addition, overlapping optical absorptions of the initiator molecules **1a**−**6a**, the radicals **1c**−**6c**, and benzoyl radicals **1b**−**6b** cause the

* Corresponding author: e-mail Mike.George@nottingham.ac.uk.
[†] University of Nottingham.
[‡] Columbia University.
[§] CLRC Rutherford Appleton Laboratory.

(1) Crivello, J. V.; Dietliker, K. *Photoinitiators for Free Radical Cationic and Anionic Photopolymerization*; John Wiley & Sons: Chichester, U.K., 1998; Vol. 3.
(2) Dietliker, K. *Radiation Curing in Polymer Science and Technology*; Elsevier Applied Science: New York, 1993; Vol. 2.
(3) Rutsch, W.; Dietliker, K.; Leppard, D.; Kohler, M.; Misev, L.; Kolczak, U.; Rist, G. *Prog. Org. Coat.* **1996**, *27*, 227−39.
(4) Herz, C. P.; Eichler, J. *Farbe Lack* **1979**, *85*, 933.
(5) Eichler, J.; Herz, C. P.; Naito, I.; Schnabel, W. *J. Photochem.* **1980**, *12*, 225−34.
(6) Jockusch, S.; Landis, M. S.; Freiermuth, B.; Turro, N. J. *Macromolecules* **2001**, *34*, 1619−26.
(7) Eichler, J.; Herz, C. P.; Schnabel, W. *Angew. Makromol. Chem.* **1980**, *91*, 39−54.
(8) Leopold, D.; Fischer, H. *J. Chem. Soc., Perkin Trans. 2* **1992**, 513−17.
(9) Rist, G.; Borer, A.; Dietliker, K.; Desobry, V.; Fouassier, J.-P.; Ruhlmann, D. *Macromolecules* **1992**, *25*, 4182−93.
(10) Ruhlmann, D.; Fouassier, J.-P.; Schnabel, W. *Eur. Polym. J.* **1992**, *28*, 287−92.
(11) Jockusch, S.; Koptyug, I. V.; McGarry, P. F.; Sluggett, G. W.; Turro, N. J.; Watkins, D. M. *J. Am. Chem. Soc.* **1997**, *119*, 11495−501.
(12) Kolczak, U.; Rist, G.; Dietliker, K.; Wirz, J. *J. Am. Chem. Soc.* **1996**, *118*, 6477−89.
(13) Martschke, R.; Farley, R. D.; Fischer, H. *Helv. Chim. Acta* **1997**, *80*, 1363−74.
(14) Jockusch, S.; Turro, N. J. *J. Am. Chem. Soc.* **1999**, *121*, 3921−25.
(15) Sluggett, G. W.; McGarry, P. F.; Koptyug, I. V.; Turro, N. J. *J. Am. Chem. Soc.* **1996**, *118*, 7367−72.
(16) Jockusch, S.; Turro, N. J. *J. Am. Chem. Soc.* **1998**, *120*, 11773−77.
(17) Huggenberger, C.; Lipscher, J.; Fischer, H. *J. Phys. Chem.* **1980**, *84*, 3467−74.
(18) Fischer, H.; Baer, R.; Hany, R.; Verhoolen, I.; Walbiner, M. *J. Chem. Soc., Perkin Trans. 2* **1990**, 787−98.

10.1021/ja026099m CCC: $22.00

kinetic analysis of the transient to be problematic. It has been demonstrated that time-resolved infrared (TRIR) spectroscopy is a powerful technique for the direct detection of benzoyl and aliphatic acyl radicals.[19−22] This is due to the fact that these radicals generally have strong ν_{CO} absorptions, in the range 1780−1880 cm^{-1}, with high extinction coefficients; e.g., for the unsubstituted benzoyl radical with $\nu_{CO} = 1828$ cm^{-1} in *n*-hexane, $\epsilon \approx 1300$ M^{-1} cm^{-1}.[22]

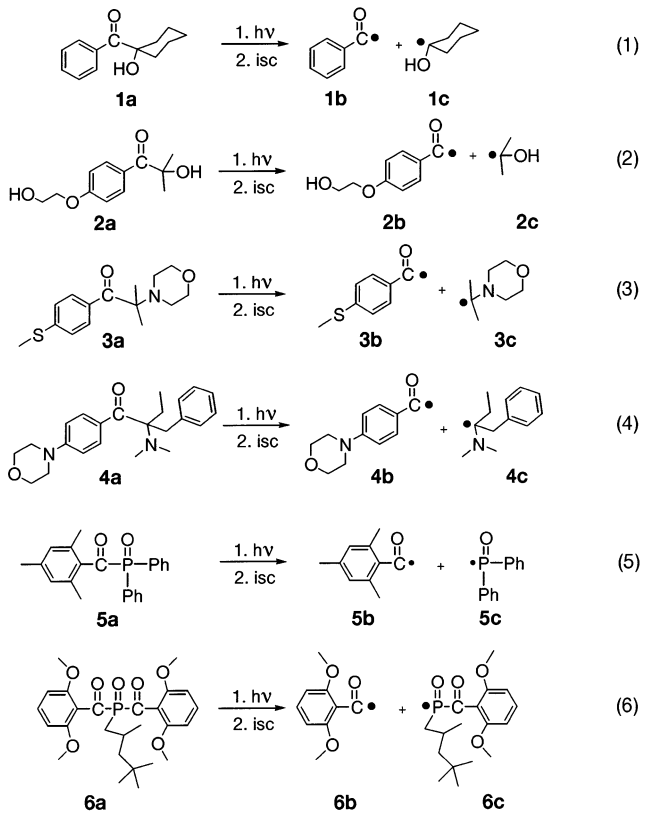

In this paper we report a systematic TRIR study of the reactivity of benzoyl radicals **1b**−**6b** toward the acrylic monomer *n*-butylacrylate and toward oxygen addition. We have also measured their reactivity toward hydrogen and bromine atom donors. The benzoyl radicals were generated by laser photolysis of photoinitators **1a**−**6a**. The photophysics and photochemistry of **5a** have been studied in detail by both nanosecond and picosecond TRIR. In addition, density functional theory (DFT) has been used in order to help elucidate some of the experimental observations.

Experimental Section

The photoinitiators, 1-hydroxycyclohexyl phenyl ketone (**1a**), 2-hydroxy-1-[4-(2-hydroxyethoxy)phenyl]-2-methyl-1-propanone (**2a**), 2-methyl-1-[4-(methylthio)phenyl]-2-(4-morpholinyl)-1-propanone (**3a**), 2-benzyl-2-(dimethylamino)-1-(4-morpholinophenyl)-1-butanone (**4a**), (2,4,6-trimethylbenzoyl)diphenylphosphine oxide (**5a**), and bis(2,6-dimethoxybenzoyl)(2,4,4-trimethylpentyl)phosphine oxide (**6a**), (all from Ciba Specialty Chemicals) were used as received and made up to concentrations ranging from 15 to 50 mM for the TRIR experiments. Sample purity was confirmed by gas chromatography/mass spectrometry (GC-MS) (>95%). Acetonitrile (Aldrich, spectrophotometric grade) was used as received.

Diode laser-based TRIR experiments, at Nottingham[23] and Columbia,[6] employed pulses from a Nd:YAG laser (Spectra Physics GCR-150-30 or GCR-12) as an excitation source. The IR probe consisted of a diode laser (Mütek MDS 1150/2) fitted with a monochromator (Mütek MDS 1400S) and sample chamber with a fast mercury cadmium telluride (MCT) detector (Kolmar Technologies KMPV11-1-J1). The signal from the detector was amplified by a low-noise preamplifier (Stanford Research Systems SR 560) and captured with a digital storage oscilloscope (Tektronix TDS 360). Argon-saturated acetonitrile solutions were flowed continuously through a 1 mm path length gastight IR cell fitted with calcium fluoride windows.

Time-resolved step-scan Fourier transform infrared (s^2-FTIR) experiments were conducted with a combination of a Nicolet Magna 860 interferometer and a Nd:YAG laser (Spectra Physics GCR-12).[24] Synchronization of the laser with data collection was achieved by use of a pulse generator (Stanford DG535). The interferometer is equipped with both an internal 100 kHz 16-bit digitizer and an external 100 MHz 12-bit digitizer (Gage 8012A). In these experiments a 1 mm photovoltaic MCT detector was used with a 20 MHz preamplifier. This detector has AC and DC outputs and both outputs are digitized simultaneously to ensure proper phase matching. The AC signal was amplified by an external preamplifier (Stanford SR 560) to use the full dynamic range of the digitizer. Single-sided interferograms were obtained from one laser pulse at each mirror position. We have used an external optical bench (Nicolet-TOM) for locating the sample cell and MCT detector. This allows easy manipulation of the UV/visible laser beam through the cell. The s^2-FTIR spectra in this paper were recorded at 8 cm^{-1} resolution with four or eight scans of the interferometer.

The ps-TRIR facility at the Rutherford Appleton Laboratory has been described in detail elsewhere.[25,26] Briefly, part of the output from a 1 kHz, 800 nm, 150 fs, 2 mJ Ti:sapphire oscillator/regenerative amplifier was used to pump a white light continuum seeded BBO OPA. The signal and idler produced by this OPA were difference frequency mixed in a type I $AgGaS_2$ crystal to generate tunable midinfrared pulses (ca. 150 cm^{-1} fwhm, 1 μJ). Second harmonic generation of the residual 800 nm light provided 400 nm pulses, which were used to excite the sample. Changes in infrared absorption were recorded by normalizing the outputs from a pair of 64-element MCT linear array detectors on a shot-by-shot basis.

DFT calculations were performed with Q-Chem software.[27] The EDF1 functional[28] was used with the 6-31+G* basis set to calculate the geometrical structure and harmonic vibrational frequencies and intensities of radicals **1b**−**6b**. EDF1 is an empirical exchange-correlation density function that was constructed with a set of accurate experimental data for calibration.[28] The justification for using this functional with the 6-31+G* basis set will not be discussed in this

(19) Vasenkov, S.; Frei, H. *J. Phys. Chem. A* **2000**, *104*, 4327−32.
(20) Sluggett, G. W.; Turro, C.; George, M. W.; Koptyug, I. V.; Turro, N. J. *J. Am. Chem. Soc.* **1995**, *117*, 5148−53.
(21) Brown, C. E.; Neville, A. G.; Rayner, D. M.; Ingold, K. U.; Lusztyk, J. *Aust. J. Chem.* **1995**, *48*, 363−79.
(22) Neville, A. G.; Brown, C. E.; Rayner, D. M.; Lusztyk, J.; Ingold, K. U. *J. Am. Chem. Soc.* **1991**, *113*, 1869−70.
(23) George, M. W.; Poliakoff, M.; Turner, J. J. *Analyst* **1994**, *119*, 551−60.
(24) Sun, X. Z.; Nikiforov, S. M.; Yang, J.; Colley, C. S.; George, M. W. *Appl. Spectrosc.* **2002**, *56*, 31−39.
(25) Towrie, M.; Bailey, P. D.; Barton, R.; Matousek, P.; Parker, A. W.; George, M. W.; Grills, D. C. Central Laser Facility, Rutherford Appleton Laboratory Annual Report 2000/2001, pp 165−67; see http://www.clf.rl.ac.uk/Report/2000-2001/pdf/75.pdf.
(26) Towrie, M.; Grills, D. C.; Dyer, J.; Weinstein, J. A.; Matousek, P.; Barton, R.; Bailey, P. D.; Subramaniam, N.; Kwok, W. M.; Ma, C.; Phillips, D.; Parker, A. W.; George, M. W. *Appl. Spectrosc.* **2002** (in press).
(27) Kong, J.; White, C. A.; Krylov, A. I.; Sherrill, D.; Adamson, R. D.; Furlani, T. R.; Lee, M. S.; Lee, A. M.; Gwaltney, S. R.; Adams, T. R.; Ochsenfeld, C.; Gilbert, A. T. B.; Kedziora, G. S.; Rassolov, V. A.; Maurice, D. R.; Nair, N.; Shao, Y.; Besley, N. A.; Maslen, P. E.; Dombroski, J. P.; Daschel, H.; Zhang, W.; Korambath, P. P.; Baker, J.; Byrd, E. F. C.; Van Voorhis, T.; Oumi, M.; Hirata, S.; Hsu, C.-P.; Ishikawa, N.; Florian, J.; Warshel, A.; Johnson, B. G.; Gill, P. M. W.; Head-Gordon, M.; Pople, J. A. *J. Comput. Chem.* **2000**, *21*, 1532−48.
(28) Adamson, R. D.; Gill, P. M. W.; Pople, J. A. *Chem. Phys. Lett.* **1998**, *284*, 6−11.

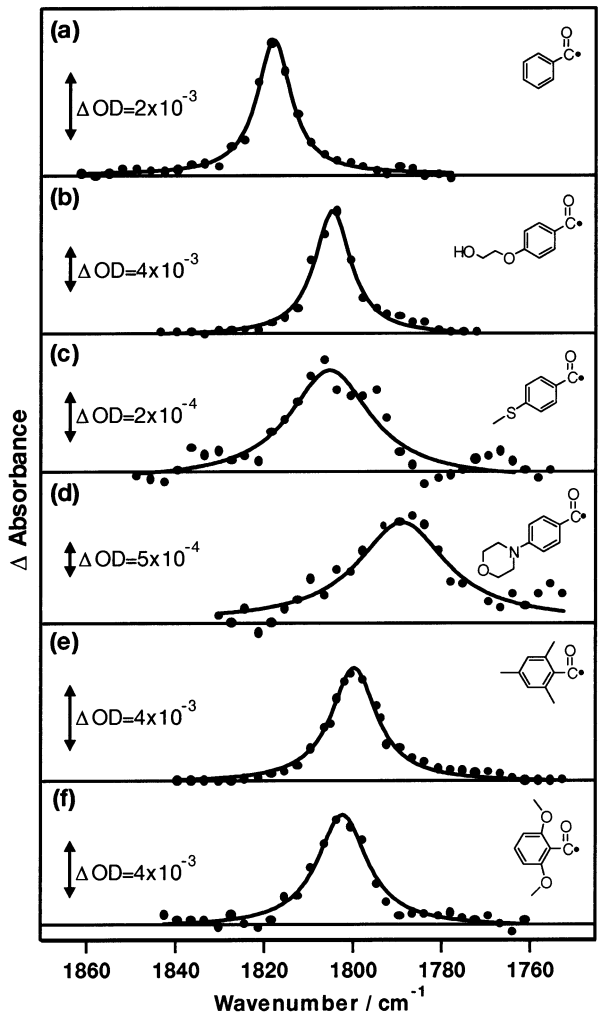

Figure 1. Diode laser-based TRIR spectra recorded 500 ns following laser excitation (355 nm, 8ns) of argon-saturated acetonitrile solutions of (a) **1a**, (b) **2a**, (c) **3a**, (d) **4a**, (e) **5a**, and (f) **6a**.

paper since this is the subject of another publication.[29] Mulliken spin populations and frontier orbital energies were calculated by use of the EDF1 functional with the 6-31G* basis set. The reason for using 6-31G* rather than 6-31+G* is that in order to calculate the spin population associated with a particular atom it is necessary to partition the electron density between the different atoms in a molecule. The + signifies that diffuse functions are included in the basis set. By definition, such functions tend to spread over a number of atoms, so that assigning electron density to particular atoms is problematic.

Results and Discussion

Figure 1 shows the diode laser-based TRIR spectra of a range of photoinitiators, **1a**−**6a**, in deoxygenated acetonitrile, obtained 500 ns following 355 nm excitation. In all cases, a transient absorption is observed between 1790 and 1820 cm^{-1}, which can be assigned to the corresponding benzoyl radicals (eqs 1−6).

Diode laser-based TRIR is an excellent technique for the characterization of benzoyl radicals since the key information can be obtained over a small spectral window. However, many problems can only be solved by obtaining data over a much wider IR region. Recent advances in s^2-FTIR, a technique that benefits from spectral multiplexing and fast data acquisition, can be used to obtain these extra data.[30]

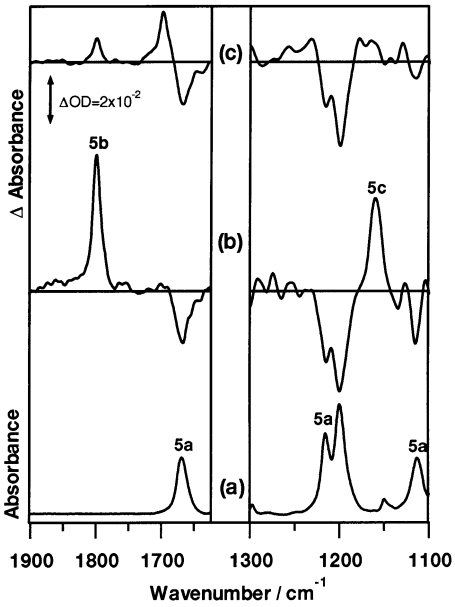

Figure 2. FTIR spectrum (a) and time-resolved s^2-FTIR spectra obtained (b) 1.1 μs and (c) 4.9 μs after laser excitation (355 nm, 8 ns) of argon-saturated acetonitrile solutions of **5a**.

As a representative example of the photoinitiators, **5a** was studied in detail by both the diode laser-based and s^2-FTIR techniques. Laser flash photolysis (λ_{ex} = 355 nm) of deoxygenated acetonitrile solutions of **5a** affords a readily detectable transient IR absorption (Figure 1e) centered at 1800 cm^{-1}, which is in good agreement with the previously published transient IR spectrum in *n*-hexane solution (ν_{max} = 1805 cm^{-1}), and which can be readily assigned to the 2,4,6-trimethylbenzoyl radical (**5b**). The transient absorption is formed within the response time of the TRIR detection system (<50 ns) and decays on the microsecond time scale with second-order kinetics ($\tau_{1/2} \approx 0.5$ μs).

s^2-FTIR has been employed to study the photochemistry of **5a** in more detail. Figure 2a shows the ground-state FTIR of **5a** in the ν_{CO} (1625−1900 cm^{-1}) and ν_{PO} (1100−1300 cm^{-1}) spectral regions in acetonitrile solution. The s^2-FTIR spectrum obtained 1.1 μs after the laser pulse (λ_{ex} = 355 nm) shows depletion of the parent bands and generation of new absorptions at 1800 and 1160 cm^{-1} (Figure 2b). The absorption at 1800 cm^{-1} is in good agreement with the transient IR spectrum recorded with diode laser-based TRIR (Figure 1e) and was assigned to the benzoyl radical **5b**. The band at 1160 cm^{-1} is tentatively assigned to the diphenylphosphinoyl radical **5c**. The s^2-FTIR spectrum obtained 4.9 μs after the laser pulse shows a decay of the two bands assigned to the radicals **5b** and **5c** and the growth of a new absorption centered at 1698 cm^{-1} (Figure 2c). This new IR absorption band is assigned to mesitil, which is formed as a secondary photoproduct by dimerization of two 2,4,6-trimethylbenzoyl radicals **5b**. This assignment has been confirmed by steady-state FTIR studies. The time evolution of the transient IR absorption is shown in Figure 3, where the decays of the radicals **5b** and **5c** and the growth of the dimerization product, mesitil, can be seen.

(29) Besley, N. A.; Colley, C. S.; Yang, J.; George, M. W.; Gill, P. M. W. Manuscript in preparation.

(30) See *Appl. Spectrosc.*, April 1997, Vol. 65, special issue on s^2-FTIR.

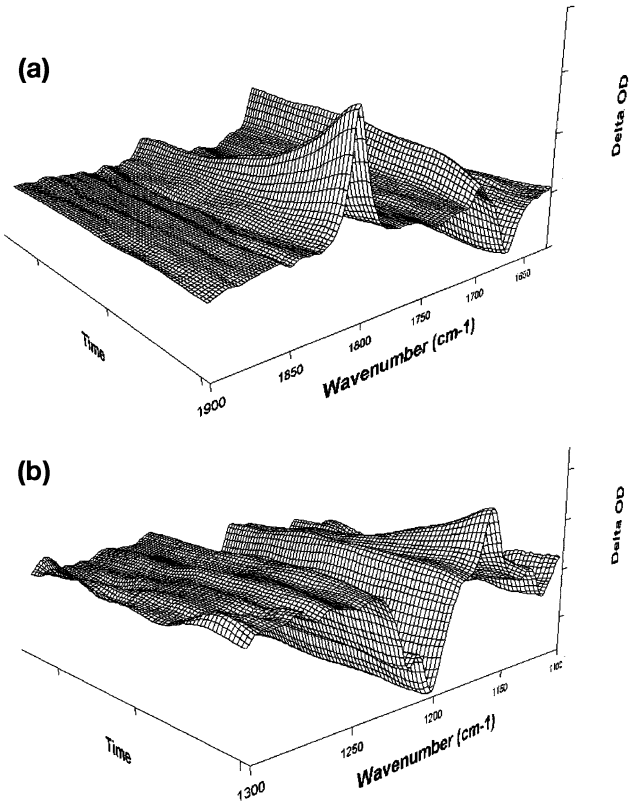

Figure 3. Three-dimensional stack plot of time-resolved s^2-FTIR spectra obtained in (a) the ν_{CO} region and (b) the ν_{PO} region, between 1 and 5 μs after laser excitation (355 nm, 8 ns) of an argon-saturated acetonitrile solution of **5a**.

TRIR and steady-state product studies of **5a** in *n*-heptane have suggested the formation of a rearrangement product (**7**) with a ν_{CO} band at 1738 cm^{-1}.[20] Since this band was seen to form within the detector response time (~50 ns) and formation of **7** was persistent in the presence of the radical quencher bromotrichloromethane ($BrCCl_3$), it was concluded that **7** is formed via in-cage recombination of radicals **5b** and **5c**. This conclusion was further supported by ^{31}P chemically induced dynamic nuclear polarization (CIDNP) studies.[12] However, in the present s^2-FTIR study, there is no evidence for the formation of **7** upon photolysis of **5a** in deoxygenated acetonitrile. This rearrangement product will be discussed in more detail later.

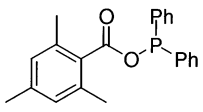

7

It is well established[11,12,31,32] that **5a** undergoes rapid α-cleavage from a triplet excited state to afford the benzoyl−phosphinoyl radical pair **5b** and **5c**, respectively (eq 5). By use of picosecond pump−probe laser flash photolysis and detection by UV absorption, the formation kinetics of the phosphinoyl radical **5c** have previously been directly observed (τ_{5c} = 123 ps).[11] The benzoyl radical **5b** could not be observed with this technique, because of the weak absorptivity in the UV spectral

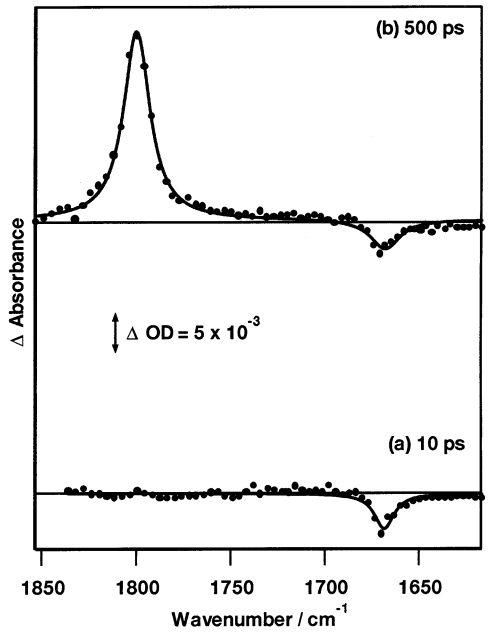

Figure 4. TRIR spectra recorded (a) 10 ps and (b) 500 ps after laser excitation (400 nm, 150 fs) of an argon-saturated acetonitrile solution of **5a**.

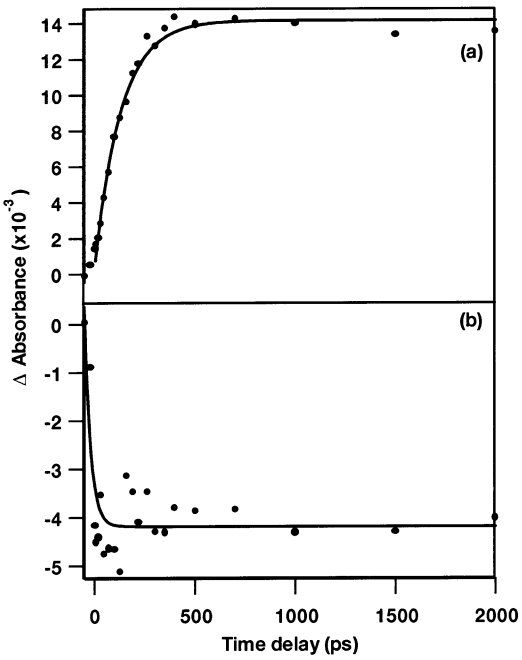

Figure 5. Transient IR absorption kinetics observed following picosecond excitation (400 nm, 1 ps) of **5a** in argon saturated acetonitrile solution, monitored at (a) 1800 cm^{-1} and (b) 1670 cm^{-1}.

range. We have therefore used ps-TRIR to elucidate the formation of **5b**. Figure 4 shows TRIR spectra recorded 10 and 500 ps after laser excitation (λ_{ex} = 400 nm) of **5a** in acetonitrile solution. In the spectral range 1600−1850 cm^{-1}, two absorption changes were observed, centered at 1670 and 1800 cm^{-1}. The kinetics at these wavenumbers are shown in Figure 5. The band at 1670 cm^{-1} corresponds to bleaching of the parent, which occurs within the response time of the instrumental setup used in these experiments (ca. 1 ps) and remains constant within the observation time window of 2 ns. Following the laser pulse, a growth of absorbance of the benzoyl radical **5b** at 1800 cm^{-1} occurs with a time constant of 130 (± 10) ps, which then

(31) Sumiyoshi, T.; Schnabel, W.; Henne, A.; Lechtken, P. *Polymer* **1985**, *26*, 141−46.
(32) Baxter, J. E.; Davidson, R. S.; Hageman, H. J.; McLauchlan, K. A.; Stevens, D. G. *J. Chem. Soc., Chem. Commun.* **1987**, 73−75.

Scheme 1. Energy Level Diagram for α-Cleavage of **5a**[a]

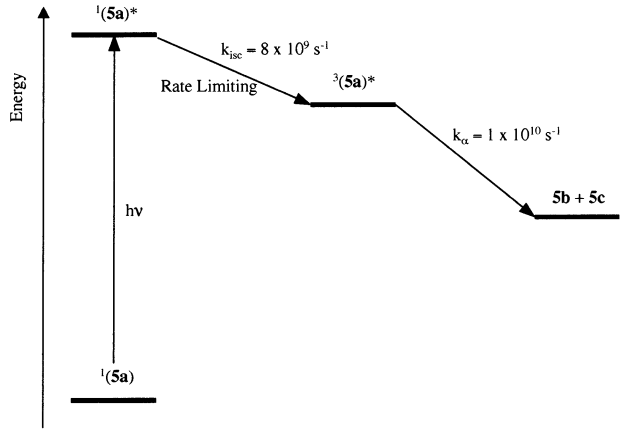

[a] See ref 11 for details.

remains constant. The kinetics of the benzoyl radical formation (**5b**, τ_{5b} = 130 ps) are in good agreement with the kinetics of phosphinoyl radical formation (**5c**, τ_{5c} = 123 ps). Moreover, the observations by ps-TRIR are entirely consistent with the mechanism for α-cleavage of **5a** proposed earlier,[11] whereby the rate-limiting step is intersystem crossing from the singlet excited state to the triplet state, and thus, the measured rate constants of growth of **5b** and **5c** represent the intersystem crossing rate constants (see Scheme 1).

It is interesting to note that this ps-TRIR experiment gives no evidence for the formation of **7** at ca. 1738 cm^{-1}. This observation is inconsistent with previous suggestions that **7** is formed via in-cage recombination of radicals **5b** and **5c**, on a subnanosecond time scale. The formation of **7** has been investigated further by diode laser-based ns-TRIR spectroscopy, and preliminary results suggest that the band at 1738 cm^{-1} is formed via a multiphoton process and is therefore only observed under conditions of high photon flux nanosecond pulses.[33]

The reactivities of the benzoyl radicals **1b**−**6b** were determined by analysis of the decay kinetics of the IR absorbance of **1b**−**6b** with the diode laser-based TRIR spectrometer following photolysis of **1a**−**6a**. For example, in argon-saturated acetonitrile solutions, laser flash photolysis (355 nm) of **5a** generated **5b**, which was monitored at 1805 cm^{-1}. This band decayed on the microsecond time scale with clean second-order kinetics ($\tau_{1/2} \approx 0.5$ μs), probably via radical−radical dimerization. In the presence of radical quenchers, such as *n*-butylacrylate, the lifetime of the benzoyl radicals decreases, due to the addition of **5b** to the olefin (eq 7).

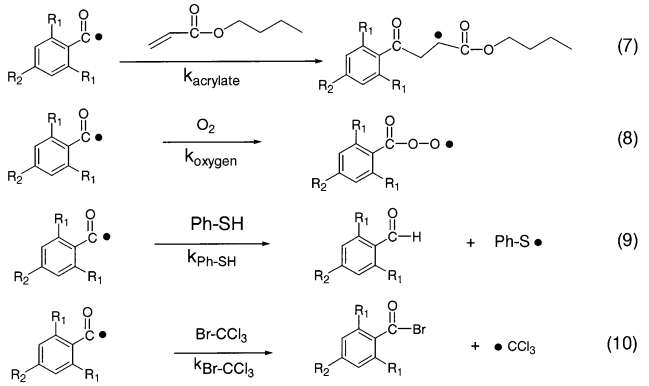

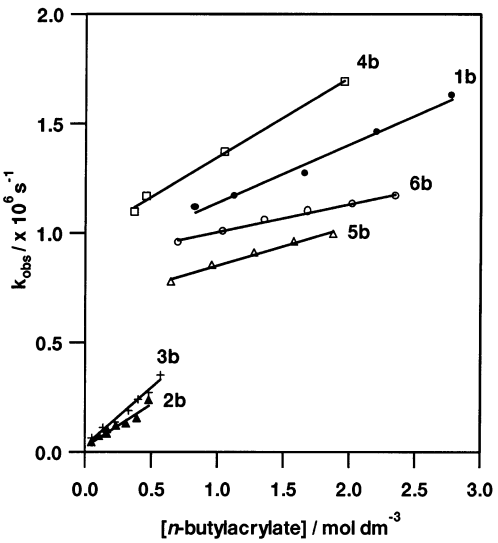

Figure 6. Pseudo-first-order decay rate constants (k_{obs}) of the benzoyl radicals **1b**−**6b** versus *n*-butylacrylate concentration, measured following laser flash photolysis (355 nm, 8 ns) of argon-saturated acetonitrile solutions of **1a**−**6a** in the presence of different *n*-butylacrylate concentrations. The rate constants for **2b** and **3b** were determined at Columbia University, and those for **1b** and **4b**−**6b**, at Nottingham.[34]

At relatively high *n*-butylacrylate concentrations, the benzoyl radical decay follows pseudo-first-order kinetics. The pseudo-first-order treatment of the decay of the IR absorbance at different *n*-butylacrylate concentrations, according to eq 11, yields the second-order rate constant $k_{acrylate}$, where k_{obs} represents the observed pseudo-first-order rate constant at various concentrations of *n*-butylacrylate and k_0 is the rate constant for the decay of the radical in the absence of added quencher (see Figure 6).

$$k_{obs} = k_0 + k_{acrylate}[\text{acrylate}] \qquad (11)$$

Similar experiments were performed for **1b**−**4b** and **6b**. The *n*-butylacrylate addition rate constants are summarized in Table 1. The $k_{acrylate}$ values that have previously[14,16] been determined for **1c**−**6c** by UV/visible flash photolysis are also included in the table for comparison. For each radical pair, the rate constant for the reaction of the benzoyl radical (**1b**−**6b**) with *n*-butylacrylate is significantly (ca. 1−2 orders of magnitude) lower than for the counterradical fragment (**1c**−**6c**).

An important common side reaction, which reduces the initiation efficiency of polymerization, is addition of oxygen to the radicals **1b**−**6b** (eq 8). The rate constants k_{oxygen} for **5b** and

(33) Following irradiation (355 nm) of **5a** in deoxygenated acetonitrile, a transient absorption is observed at ca. 1734 cm^{-1} with diode laser-based TRIR, suggesting the formation of **7**. However, an experiment has been performed in which the intensity (Δabsorbance) of the 1734 cm^{-1} band has been monitored as a function of laser pulse fluence. The relationship between Δabsorbance and pulse energy has been found to be nonlinear. A plot of ln (Δabsorbance) vs ln (laser energy) has been fitted to a straight line with a gradient of ca. 2−3, strongly suggesting that formation of **7** is a multiphoton process. Therefore, this result provides a possible explanation for the absence of a band at ca. 1734 cm^{-1} in the s^2-FTIR and ps-TRIR experiments, where the UV laser energy is lower than in the diode laser-based TRIR experiment. Observation of **7** is possible with diode laser-based TRIR since there is sufficient UV photon fluence to pump the multiphoton process.

(34) The TRIR kinetic experiments at Columbia and Nottingham were carried out under slightly different conditions of laser power and photoinitiator concentration. This accounts for the differences in k_0 obtained from the fits to these data. However, the slopes of the lines ($k_{acrylate}$) will be unaffected and are therefore directly comparable. The kinetics of *n*-butylacrylate addition to **4b** were measured in both laboratories, giving identical rate constants.

Table 1. ν_{CO} Frequencies and Bimolecular Rate Constants[a] for Reactions of Benzoyl Radicals (**1b**−**6b**) and Their Counterradicals (**1c**−**6c**)

radical	ν_{CO} (cm^{-1})	$k_{acrylate}$ ($M^{-1}\,s^{-1}$)	k_{PhSH} ($M^{-1}\,s^{-1}$)	k_{BrCCl_3} ($M^{-1}\,s^{-1}$)	k_{O_2} ($M^{-1}\,s^{-1}$)
1b	1818	2.7×10^5	1.8×10^7	1.8×10^8	
1c		1.3×10^7 [b]			5.4×10^9 [b]
2b	1805	3.5×10^5			
2c		1.3×10^7 [b]			6.6×10^9 [b]
3b	1805	5.5×10^5			
3c		6.1×10^6 [b]			4.3×10^9 [b]
4b	1789	3.6×10^5	5.4×10^7	5.8×10^8	
4c		6.1×10^6 [b]			4.3×10^9 [b]
5b	1800	1.8×10^5	3.9×10^6		3.0×10^9
5c		2.8×10^7 [c]	4.2×10^6 [c]	6.9×10^8 [c]	4.2×10^9 [c]
6b	1803	1.3×10^5	7.1×10^6	1.1×10^8	3.3×10^9
6c		1.5×10^7 [c]		2.4×10^8 [c]	2.6×10^9 [c]

[a] Reactions with *n*-butylacrylate, thiophenol, bromotrichloromethane, and oxygen in acetonitrile solution at 298 K were performed. Rate constant values are ±10%. [b] Reference 14. [c] Reference 16.

6b were determined by monitoring the radical decay as a function of oxygen concentration (0.85−3.4 mM). The variable oxygen concentrations were achieved by saturation of the acetonitrile solutions with air at different pressures. Determination of k_{oxygen} for **6b** was more complex. The absorption assigned to the benzoyl radical decayed with double-exponential kinetics. The slower exponential decay was independent of oxygen concentration, whereas the faster exponential decay was found to be dependent on the oxygen concentration. These double-exponential decay kinetics can be explained in terms of a spectral overlap between the benzoyl radical and the benzoyl peroxy radical, which is the addition product of oxygen to the benzoyl radical (eq 8).

Other common reactions, which reduce the initiation efficiency of polymerization, are atom abstractions from materials that are required to be present in a photocuring formulation. To distinguish the reactivity between the different benzoyl radicals toward atom abstraction, we chose model compounds with high atom donor tendencies, i.e., thiophenol (PhSH) and bromotrichloromethane ($BrCCl_3$). The k_{PhSH} values determined for **1b**, **4b**, **5b**, and **6b** and the k_{BrCCl_3} values determined for **1b**, **4b**, and **6b** are shown in Table 1. Measurement of the rate constant for addition of **5b** to $BrCCl_3$ has been attempted but the kinetics were more complicated.[35] A previously measured k_{PhSH} value for **5c** and k_{BrCCl_3} values for **5c** and **6c** are also included in the table. For each benzoyl radical, k_{PhSH} is approximately 1 order of magnitude less than k_{BrCCl_3}. This observation is consistent with previous work,[15,20] which has identified a qualitative relationship between the rate constant and the strength of the bond that is broken in the atom donor: $BrCCl_3$ (56 kcal mol^{-1}) > PhSH (75 kcal mol^{-1}). In contrast to the reactivity toward *n*-butylacrylate, the atom abstraction rate constants for each radical fragment within a radical pair appear to be strikingly similar to each other (e.g., $k_{PhSH} = 3.9 \times 10^6$ M^{-1} s^{-1} for **5b** and 4.2×10^6 M^{-1} s^{-1} for **5c**). It has been suggested[20] that this implies that the transition states for additions of, e.g., **5b** and **5c** to unsaturated compounds, such as *n*-butylacrylate, may be situated slightly further along the reaction coordinate than the transition states for atom abstraction reactions, and thus steric and electronic effects are more important.

(35) Even at low $BrCCl_3$ concentrations, the kinetic trace at 1800 cm^{-1} decayed to a residual absorption. With increasing $BrCCl_3$ concentration, the amount of residual absorption increased further. In an attempt to understand this kinetic behavior, the s^2-FTIR spectrum of **5a** was measured in deoxygenated acetonitrile, in the presence of 5 mM $BrCCl_3$. It was found that the product of the atom abstraction, trimethylbenzoyl bromide, has a ν_{CO} band at 1800 cm^{-1}, which overlaps with **5b**. However, the mechanism of formation of trimethylbenzoyl bromide is unclear since its yield is highly dependent upon the concentration of $BrCCl_3$. Furthermore, a new photoproduct with a strong absorption at ca. 1734 cm^{-1} was observed only when $BrCCl_3$ was present. This is consistent with the formation of the rearrangement product **7** during these trapping experiments. The precise mechanism is still unclear and further experiments are in progress to fully understand this process.

Table 2. Experimental and Calculated ν_{CO} Frequencies, Calculated Carbonyl C and P Atom Mulliken Spin Population (MSP) Values, and $\Delta E_{acrylate}$ for Radicals **1b**−**6b**, **5c**, and **6c**

radical	ν_{CO} expt (cm^{-1})	νCO calc (cm^{-1})	MSP carbonyl C or P (au)	calcd ΔE_{HOMO} (au)	calcd ΔE_{LUMO} (au)	calcd ΔE_{total} (au)
1b	1818	1813	0.64	5.8	5.8	11.6
2b	1805	1807	0.65	5.3	6.5	11.8
3b	1805	1806	0.65	5.4	6.4	11.8
4b	1789	1795	0.65	4.8	7.7	12.5
5b	1800	1800	0.64	4.6	7.1	11.7
6b	1803	1812	0.65	4.1	10.0	14.1
5c			0.48	4.5	2.5	7.0
6c			0.42	3.1	2.0	5.1

Density functional theory (DFT) has been used in order to give further insight into these experimental results. Table 2 shows that there is very good agreement between the experimental and DFT calculated IR frequencies. However, it should be noted that this agreement (average difference between experiment and theory is ±3.8 cm^{-1}) may be somewhat fortuitous since the IR spectra are calculated for an isolated single molecule, whereas the experimental spectra are measured in a polar solvent. Experimentally the ν_{CO} frequencies decrease in the order **1b** > **2b** ≈ **3b** > **6b** > **5b** > **4b** but the calculated ν_{CO} frequencies decrease in the order **1b** > **6b** > **2b** > **3b** > **5b** > **4b**. Thus, it appears that the ν_{CO} frequency calculated for **6b** is slightly too high relative to the other radicals. A possible reason for this is that in **6b** two different local minima can be attained: one in which the two methyl groups are eclipsed in the plane of the aromatic ring and another in which they are staggered in the plane of the ring. The calculations show that the barrier for reorientation of the methyl groups is relatively small. The ν_{CO} frequencies were found to be sensitive to the conformation (eclipsed conformation, $\nu_{CO} = 1812$ cm^{-1}; staggered conformation, $\nu_{CO} = 1795$ cm^{-1}).

This agreement between the experimental and theoretical ν_{CO} frequencies provides some confidence that the EDF1 density functional adequately describes the electronic structure of the radicals. A number of factors will govern the reactivity of the radicals **1b**−**6b**, including steric, entropic, and electronic effects. DFT calculations can provide information about the electronic structure of the radicals that cannot be obtained experimentally. Consequently, it is of interest to see if DFT can rationalize and potentially predict the reactivities of the radicals. While factors such as steric effects are difficult to quantify, they can often be regarded as constant when comparing the reactivities of a number of sterically similar radicals. The extent to which the orbitals of two reacting molecules can affect the rate of a reaction can be estimated by perturbation theory. This interaction can be considered to raise or lower the barrier to reaction. The change in the barrier height is given by[36]

$$\Delta E = \sum_{r}^{occ}\sum_{s}^{unocc} - \sum_{s}^{occ}\sum_{r}^{unocc} \frac{2\left(\sum_{ab} c_{ra} c_{sb} \beta_{ab}\right)^2}{E_r - E_s} \qquad (12)$$

where c_{ra} is the coefficient of atomic orbital a in molecular orbital r, where r refers to the molecular orbitals on one molecule and s refers to the molecular orbitals on the other, β_{ab} is the resonance integral, and E_r is the energy of molecular orbital r. The greater ΔE is, the more the reaction barrier is lowered and consequently the rate increased. In a frontier orbital picture of the reaction between a radical and molecule, only the interaction between the SOMO (singly occupied molecular orbital) of the radical and both the HOMO (highest occupied molecular orbital) and LUMO (lowest unoccupied molecular orbital) of the reacting molecule are considered. If the resonance integral is assumed to be constant for all the radicals, then a measure of the relative changes in ΔE_{HOMO} can be estimated by

$$\Delta E_{HOMO} = \frac{MSP^2}{|E_{HOMO} - E_{SOMO}|} \quad (13)$$

and similarly for ΔE_{LUMO} where MSP is the Mulliken spin population of the carbonyl carbon. If ΔE_{HOMO} is significantly greater than $\Delta E_{LUMO,}$ then the reaction involving the SOMO and the HOMO will be favored, and similarly, if ΔE_{LUMO} is greater the SOMO will interact with the LUMO.

The electron spin density is a complicated function of position and it is conceptually helpful to partition it into atomic components. Unfortunately, because there is no rigorous quantum mechanical definition of an atom within a molecule, a unique partition does not exist and it is necessary to adopt one of the many alternative schemes that have been suggested over the years. One of the most popular of these, and the one that we have chosen, is the Mulliken spin population analysis. Although it is not a sophisticated method, the assumptions of Mulliken analysis are consistent with those of the semiquantitative frontier molecular orbital theory that we use. Table 2 shows the calculated MSP on the carbonyl C atom, ΔE_{HOMO}, and ΔE_{LUMO} of **1b**−**6b** for the reaction with *n*-butylacrylate. There appears to be little difference in MSP values between the radicals **1b**−**6b**. This is in agreement with the experimental results where a similar reactivity of **1b**−**6b** was found. The observed small difference in reactivity of **1b**−**6b** probably does not arise from a large variation in the spin density at the carbonyl C atom. However, ΔE_{HOMO} and ΔE_{LUMO} do provide some insight into the changing nature of the reaction. For **1b** the interactions of the SOMO with the HOMO and LUMO are found to be equivalent. However, for **2b**−**6b** the calculations suggest that there is an increasing tendency for reaction via the LUMO. It is probably too much to expect this type of relatively simple analysis to provide accurate predictions of the relative rates of these reactions. However, the calculations generally agree with experiment. The major anomaly is **6b**, which is predicted to have the fastest rate, and for this radical steric effects may be important. To model these effects requires more detailed calculations examining the transition states of the reactions. It should be noted that the Mulliken spin populations were found to be largely insensitive to changes in molecular conformation.

(36) Fleming, I. *Frontier Orbitals and Organic Chemical Reactions*; John Wiley & Sons: Chichester, U.K., 1978.

Time-resolved electron spin resonance spectroscopy (TR-ESR) has been previously used to study phosphinoyl radicals, including **5c** and **6c**.[15,16] The high reactivity of phosphinoyl radicals has been attributed to a high degree of s-character and spin localization on the P atom. These characteristics are reflected by large ^{31}P hyperfine coupling constants (hfcc) in the TR-ESR spectra, which provides an experimental indicator of the extent of spin localization. The lower ^{31}P hfcc of **6c** (^{31}P hfcc = 286 G) compared with **5c** (^{31}P hfcc = 369 G) indicates that the P atom of **6c** possesses a lower degree of spin localization, which is considered to result in the lower reactivity toward unsaturated compounds and atom donors. The calculated P atom MSPs for radicals **5c** and **6c** are 0.48 and 0.42, respectively, which agree with the experimental observations where there is a significant difference in reactivity between these radicals. Furthermore, the computed ΔE_{total} values indicate that this does result in a greater rate. It should be noted that the computed ΔE_{total} for the phosphinoyl radicals should not be compared to those for the benzoyl radicals since eq 13 is only valid for comparisons between similar radicals.

Conclusions

A series of substituted benzoyl radicals (**1b**−**6b**) have been generated by laser flash photolysis of α-hydroxy ketones (**1a**, **2a**), α-amino ketones (**3a**, **4a**), and acyl and bis(acyl)phosphine oxides (**5a** and **6a**, respectively). The benzoyl radicals were characterized by TRIR in acetonitrile solution and their absolute rate constants for addition to *n*-butylacrylate, thiophenol, bromotrichloromethane, and oxygen were determined. The rate constants of benzoyl radical addition to *n*-butylacrylate range from 1.3×10^5 to 5.5×10^5 M^{-1} s^{-1}. DFT calculations have been used to rationalize the relative rates of these reactions. These calculations show that from **1b** to **6b** there is an increasing tendency of the radical to react via the LUMO of *n*-butylacrylate. The rate constants for *n*-butylacrylate addition to radicals **1b**−**6b** are about 2 orders of magnitude lower than for the counterradicals (**1c**−**6c**), suggesting that the benzoyl radicals are less efficient in initiation of free radical polymerization. Analysis of the spin population at the phosphorus atom supports previous experimental observations of TR-ESR spectra that greater localization of the spin on the phosphorus atom results in faster rates. The experiments outlined in this paper have demonstrated the power of TRIR to probe photopolymerization initiation. Further work is in progress to fully elucidate the propagation steps following the initiation process by use of TRIR.

Acknowledgment. The authors at Columbia thank the National Science Foundation and Ciba Specialty Chemicals, Inc., for their generous support of this research and Dr. M. Kunz (Ciba Specialty Chemicals) for samples **1a**−**6a**. The authors at Nottingham thank the EPSRC and Nicolet Instruments for financial support. We are especially grateful to Dr. C. Hayes for many helpful discussions.

Supporting Information Available: Equilibrium geometries of radicals **1b**−**6b**, **5c**, and **6c** (PDF). This material is available free of charge via the Internet at http://pubs.acs.org.

JA026099M